

## Exploiting Force Sensitive Spiropyrans as Molecular Level Probes

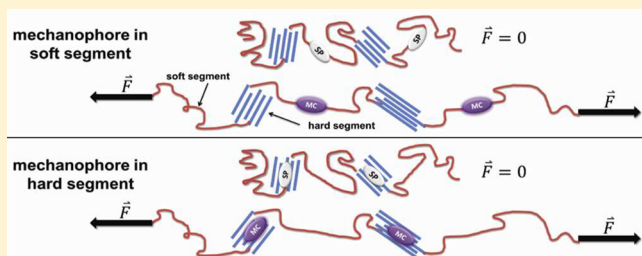
Corissa K. Lee, Brett A. Beiermann, Meredith N. Silberstein, Joanna Wang, Jeffrey S. Moore, Nancy R. Sottos, and Paul V. Braun\*

Department of Materials Science and Engineering, Beckman Institute for Advanced Science and Technology, Department of Chemistry, University of Illinois at Urbana-Champaign, Urbana, Illinois 61801, United States

### Supporting Information

**ABSTRACT:** Spiropyran (SP) mechanophore was synthesized into the soft or hard phase of segmented polyurethanes (SPU) and used as a molecular probe of force and orientation. Upon either tensile stretching or irradiation with UV light the SP-linked segmented polyurethane (SP-SPU) adopt a deep purple coloration and are fluorescent, demonstrating the force and UV-induced formation of the open merocyanine (MC) form of the mechanophore. Order parameters calculated from the anisotropy of the fluorescence polarization of merocyanine (MC) were used to characterize the orientation in each phase.

Exploiting the ability of SP to be force activated, the SP-SPUs were also mechanically activated to track the force and orientation in each domain of segmented polyurethane during uniaxial tensile loading.



### INTRODUCTION

Mechanochemistry<sup>1</sup> is a growing field of the study of force-induced productive chemical reactions. A considerable fraction of the research in mechanochemistry focuses on molecules that respond to external mechanical forces; such molecules are defined as mechanophores.<sup>2,3</sup> To date, a number of mechanophores have been developed which demonstrate force-triggered functionalities including color change,<sup>4,5</sup> generation of reactive moieties,<sup>6–8</sup> and catalyst release.<sup>9,10</sup> While much attention has been focused on using mechanophores to add functionality to polymers, their inherent mechanochemical changes take place on the molecular scale making them attractive as localized force probes. Here we exploit the ability of a spiropyran mechanophore to react to local forces and demonstrate its use as a spatially sensitive molecular probe in segmented polyurethane.

Spiropyran (SP), a popular mechanophore, is a well-characterized molecule which undergoes a reversible 6- $\pi$  electrocyclic ring-opening reaction to a merocyanine (MC) form<sup>11</sup> (Figure 1). The SP mechanophore was first incorporated into solid state polymers by Davis et al.,<sup>5</sup> who demonstrated stress-induced ring-opening of the SP within poly(methyl acrylate) (PMA) into the highly colored and fluorescent MC form. More recently, mechanochemical reactivity of SP has been demonstrated in a number of different polymer systems,<sup>5,12–15</sup> adding to the understanding of how time<sup>13</sup> and mobility<sup>12,14</sup> play important roles in the transmission of macroscopic force to these reactive moieties. Beiermann et al.<sup>16</sup> used the fluorescence anisotropy of MC<sup>17</sup> in PMA (elastomeric) and poly(methyl methacrylate) (PMMA) (glassy) to characterize the role of orientation in mechanically activating SPs. Results showed that force-induced activation correlates to the mechanophore's state of alignment

relative to the tensile direction. The fluorescence anisotropy method of characterizing SP mechanophore orientation is promising for probing orientation and force in distinct environments of a more complex polymer system, such as phase-separated segmented polyurethane (SPU).

Polyurethanes are of particular interest not only because of their many useful engineering properties but also due to their highly tunable mechanical properties, which enables a study on the effect of mechanics on mechanochemistry in a single class of polymers.<sup>18</sup> Polyurethanes have high abrasion and chemical resistance, excellent mechanical and elastic properties, and are blood and tissue compatible.<sup>19</sup> The typical segmented polyurethane elastomer is a linear block copolymer containing three primary components: a polyol, a diisocyanate, and a chain extender resulting in polymers of alternating hard (isocyanate and chain extender) and soft (long chain polyols) segments. It is well recognized that the impressive combination of the elasticity and strength of segmented polyurethanes is in large part due to the two-phase nature of these materials. The thermodynamic incompatibility of the chemically distinct hard and soft segment microphase segregates into separate soft and hard segment domains. With increasing hard segment content the elastic modulus and degree of phase segregation both increase.<sup>20</sup> It is therefore of particular interest to study and understand how force is distributed over this two-phased morphology for a wide range of strain levels.

In part for the reasons described above, polyurethanes have been popular polymers for the incorporation and study of mechanochromic moieties. Rubner<sup>21,22</sup> first studied the color

Received: March 13, 2013

Revised: May 3, 2013

Published: May 14, 2013



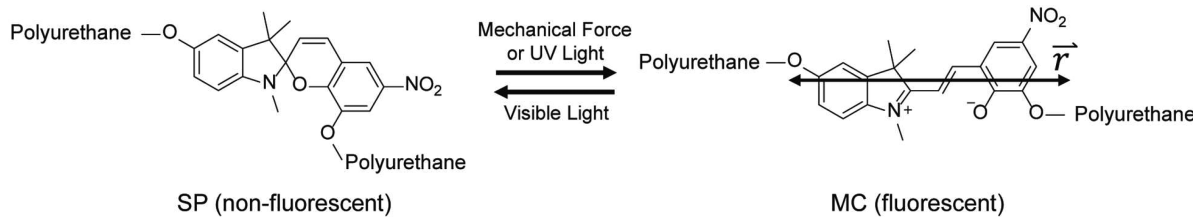


**Figure 1.** Ring-opening of SP to MC, with approximate MC transition dipole ( $\vec{r}$ ).

changing optical properties of polydiacetylene in a segmented polyurethane and reported on its thermochromic and mechanochromic properties. Since then, other reports<sup>23–26</sup> have described the use of mechanochromic polydiacetylenes to study the organization and role of the hard segment domains in segmented polyurethane during tensile deformation. Kim et al.<sup>37</sup> used the trans-to-cis isomerization of diaminoazobenzenes synthesized into segmented polyurethane as a “strain recording material”. Most recently, Crenshaw and Weder<sup>28,29</sup> blended and covalently incorporated cyano-substituted oligo(*p*-phenylenevinylene) (cyano-OPV) into segmented polyurethane. Mechanical deformation of these systems led to irreversible phase separation exhibiting corresponding photoluminescent color change. Recently, we reported on the synthesis and properties of SP-linked polyurethane (not segmented).<sup>13</sup> Here, using a similar step growth polymerization approach, a segmented polyurethane containing the SP mechanophore in either the soft or the hard segment is synthesized. The SP mechanophore’s sensitivity to molecular level forces will be used to probe each phase of segmented polyurethane during uniaxial tensile loading, providing information about the force and the molecular alignment within each phase.

## EXPERIMENTAL SECTION

**Materials.** 1,6-Hexamethylene diisocyanate (HDI), 4,4'-methylenebis(phenyl isocyanate) (MDI), poly(tetramethylene oxide) (PTMO) ( $M_n \approx 1000$  g/mol), 1,4-butanediol (BD), and 1,4-diazabicyclo[2.2.2]octane (DABCO) were purchased through Sigma-Aldrich. The PTMO and BD were dried under high vacuum at 70 °C for 1–2 h before use. Hydroxyl-functionalized spiropyran (SP) was synthesized according to the procedure outlined by Davis et al.<sup>5</sup> Anhydrous tetrahydrofuran (THF) was obtained from an Anhydrous Engineering Solvent Delivery System (SDS) equipped with activated alumina columns. Reactions were performed under a N<sub>2</sub> atmosphere unless otherwise specified.

**SP Functionalization.** Dihydroxy-functionalized SP (3 mg, 8.5 μmol) and DABCO (8 mg, 71 μmol) were dissolved in anhydrous THF (5 mL) to form solution A. MDI (125 mg, 0.5 mmol) was dissolved in an equal volume of anhydrous THF to form solution B. A large molar excess of MDI to SP was used to ensure diisocyanate functionalization of the SP and to minimize the probability of SP-MDI oligomerization. Solution A was added dropwise to solution B, mixed, and heated at 70 °C for 1 h.

**SP in the Soft Segment (SPSS).** For the 40 wt % hard segment SPU the functionalized SP solution was added to the PTMO soft segment (4.89 g, 4.89 mmol). While the SP mechanophore reacted with the PTMO at 70 °C, the THF solvent was simultaneously removed under high vacuum. Next, HDI (2.31 g, 13.76 mmol) was added to the PTMO and reacted at 70 °C for 2 h. Finally the hard segment chain extender BD (0.8 g, 8.88 mmol) was added, thoroughly mixed, degassed, poured into Delrin “dog-bone”-shaped molds, and cured in an N<sub>2</sub>-purged oven at 60 °C for 2 days. The 22 wt % hard segment SPU was synthesized using the above procedure with the ratio of monomers as follows: PTMO:HDI:BD 6.25:8.92:2.66 mmol.

**SP in the Hard Segment (SPHS).** For the 40 wt % hard segment SPU, the functionalized SP solution was added to BD (0.8 g, 8.88

mmol) and reacted for 10–15 min. The SP-BD solution was then added to a soft segment prepolymer of PTMO (4.89 g, 4.89 mmol), HDI (2.31 g, 13.76 mmol), and DABCO (2 mg, 18 μmol) presynthesized for 1.5–2 h at 70 °C. While reacting, the polymer was put under high vacuum to remove the THF solvent. Finally, the polymer was poured into Delrin “dog-bone”-shaped molds and cured in an N<sub>2</sub>-purged oven at 60 °C for 2 days. The 22 wt % hard segment SPU was synthesized using the above procedure with the ratio of monomers as follows: PTMO:HDI:BD 6.25:8.92:2.66 mmol.

**Sample Preparation.** For UV activated experiments SPU samples were irradiated with UV light ( $\lambda = 365$  nm) for 10 min immediately prior to mechanical testing and imaging. For mechanically activated experiments a halogen light source was used to irradiate visible light on the SPU samples for at least 10 min to drive the equilibrium toward the nonfluorescent SP form. This was to ensure that mechanically activated mechanophore in the fluorescent MC form would dominate the fluorescence response.

**Optical Characterization.** A circularly polarized 532 nm laser was used to excite the fluorescent SPU samples. Full field fluorescence was collected using a CCD camera (Allied Vision Technology model 145C) after passing through a linear polarizer positioned either parallel or perpendicular to the stretch direction. The red channel intensity of the CCD, corrected for background noise, was taken as the fluorescence intensity. The fluorescence intensities were averaged over each CCD pixel to calculate an order parameter. A schematic of the experimental setup for fluorescence anisotropy collection was previously reported<sup>16</sup> and can be found in the Supporting Information (Figure S1).

**Mechanical Testing.** SPU samples were strained incrementally, with steps of 25% strain with respect to the initial length, at a strain rate of 0.004 s<sup>-1</sup> using a bidirectional screw driven rail table. Force was measured using a Honeywell Sensotech load cell with load capacity of 220 N. Between each motion step, a fluorescent image was taken with a linear polarizer in either the parallel or perpendicular orientation, the polarizer was then rotated 90°, and a fluorescent image was taken at the second polarizer orientation. The elongation was reported using a stretch ratio ( $\lambda$ ), defined as the final length over the initial length. True stress is defined assuming incompressibility as

$$\sigma_{\text{true}} = \frac{P}{A_0} \quad (1)$$

where  $P$  is defined as the load,  $A_0$  is the initial cross-sectional area, and  $\lambda$  is the stretch ratio.

**Order Parameter.** The relative orientation was determined using an order parameter ( $S$ ) based on the second-order Legendre polynomial  $P_2$ :

$$\langle P_2 \rangle = \frac{\langle 3 \cos^2(\beta) - 1 \rangle}{2} \equiv S \quad (2)$$

where  $\beta$  is the angle between the stretch direction and the predominant emission dipole moment ( $\vec{r}$ ) of the MC molecule (Figure 1). From eq 2, order parameter values vary between 0 (random distribution) and 1 (perfect alignment). The order parameter is derived from eq 2 based on the measured parallel and perpendicular fluorescence intensities with respect to the stretch direction:<sup>31,32</sup>

$$S = \frac{I_{||} - I_{\perp}}{I_{||} + 2I_{\perp}} \quad (3)$$

where  $I_{\parallel}$  and  $I_{\perp}$  represent the total fluorescence intensity with the linear polarizer parallel and perpendicular to the stretch direction, respectively. Equation 3 assumes that the mechanophore is rotationally fixed during each set of parallel and perpendicular measurements.

**Optical Corrections.** Fluorescence images of SPU samples after visible light exposure and under no load showed a small level of inherent fluorescence. The inherent fluorescence is a result of a small population of mechanophore in the MC form at equilibrium in SPU ( $I_{eq}$ ). While the equilibrium form of the mechanophore is predominantly the colorless SP constitution,<sup>13</sup> this small population of randomly oriented MC prior to stretching lowers the calculated “mechanically activated” order parameter. We define the measured fluorescence intensity as the sum of fluorescence from mechanically activated mechanophore ( $I_{mech}$ ) and the mechanophore in the MC form at equilibrium ( $I_{eq}$ ).

$$I_{meas} = I_{mech} + I_{eq} \quad (4)$$

To determine order parameters for only mechanically activated mechanophore, the measured fluorescence intensity ( $I_{meas}$ ) is first corrected for the inherent fluorescence and scattering due to changes in sample thickness during testing using experimental data collected from a nonmechanically activated difunctional control SP mechanophore<sup>5,13</sup> synthesized into SPU (see Figure S2 for detailed chemistry). Its fluorescence behavior with stretch was measured, and  $T_{correction}$  is defined as the normalized fluorescence intensity from the difunctional control SP in SPU during stretching seen in Figure 4 (“22 wt % Control” and “40 wt % Control”). The measured fluorescence with the correction factor is defined in eq 5.

$$\frac{I_{meas}}{T_{correction}} = I_{mech} + I_{eq}(1 - x) \quad (5)$$

$T_{correction}$  is the thickness and scattering correction factor and  $x$  is the fraction of mechanophore which mechanically activate relative to the total concentration of mechanophore. From previous studies<sup>13</sup> we can assume that the number of mechanically activated mechanophore is low compared to the total concentration of mechanophore, and therefore this term is dropped and the fluorescence correction equation, solving for  $I_{mech}$ , can be approximated as

$$I_{mech} = \frac{I_{meas}}{T_{correction}} - I_{eq} \quad (6)$$

Equation 6 is applied to the measured fluorescence data of all mechanically activated tests, and the order parameters were calculated using  $I_{mech}$  values. While the resulting order parameters are a more accurate representation of mechanically activated mechanophore orientation, the equation does not account for the orientation effects on  $I_{eq}$  at different stretch ratios (the effect of strain on the angular distribution of the equilibrium population of mechanophores in the MC form). We simply assume any changing orientation of  $I_{eq}$  at different stretch ratios is negligible for this correction. This assumption is supported by the UV activated data seen in Figure 5 where the order parameter of the initially randomly oriented SP even at the maximum stretch ratio is relatively low (0.1–0.3).

**Differential Scanning Calorimetry.** Thermal properties of the SPUs were determined using differential scanning calorimetry (DSC) with a Mettler-Toledo model DSC821. Each sample was first heated from room temperature (25 °C) to 200 °C and then cycled from −150 to 200 °C at 20 °C min<sup>−1</sup>.

## RESULTS AND DISCUSSION

**SPU Characterization and Activation.** Segmented polyurethane (SPU) with spiropyran (SP) mechanophore (SP-SPU) incorporated into either the soft segment (SPSS) or hard segment (SPHS) was synthesized at a low (22 wt %) and high (40 wt %) hard segment (HS) composition. Thermal analysis using DSC shows a soft segment glass transition temperature ( $T_g$ ) of ca. −70 °C for both hard segment compositions (Figure 2). In the 40 wt % sample, there is a clear

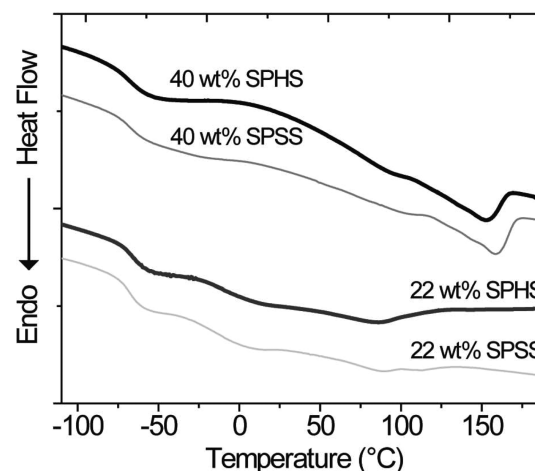


**Figure 2.** DSC curves (second heating) of low (22 wt %) and high (40 wt %) hard segment content SPU of SPSS and SPHS.

hard domain melting endotherm at  $T_m$  ca. 160 °C, while in the 22 wt % sample the melting endotherm is shifted to a lower temperature and is broader ( $T_m$  ca. 85 °C). The literature  $T_m$  of pure HDI-BD hard segment is 180 °C,<sup>33</sup> so the shifted  $T_m$  in the 22 wt % material is most likely due to partial miscibility of hard and soft segments at this lower hard segment content.<sup>34</sup> The location of the SP does not measurably influence  $T_g$  or  $T_m$  in either material (Figure 2).

Stress–stretch curves are presented in Figure 3. As expected, higher hard segment content increases stiffness and strain

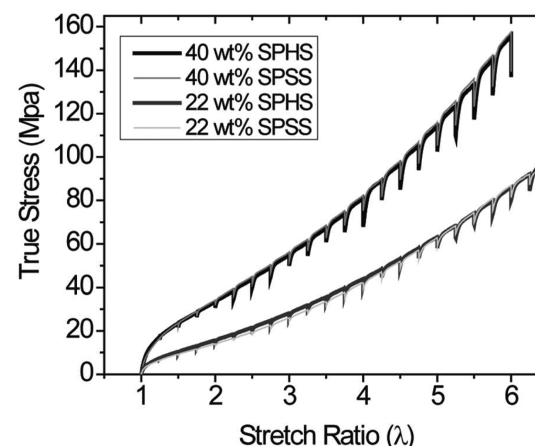


**Figure 3.** Typical step loading stress vs stretch ratio curves of the low (22 wt %) and high (40 wt %) hard segment compositions with the SP incorporated in either the hard segment (SPHS) or the soft segment (SPSS).

hardening response. Drops in the stress are due to polymer relaxation at each stop in deformation to capture the fluorescence images. The relaxation appears to be minimal, and the overall stress in the SPU is comparable to SPU stretched at a continuous strain rate (see Figure S3 in Supporting Information). The location of the SP (incorporation into the hard or soft segment) does not induce statistically significant changes in the mechanical behavior of the material. The lack of change enabled direct SP-based comparisons of the two segments within each material.

When the SP-SPU was stretched monotonically, the coloration of the polymer changed to a deep purple due to

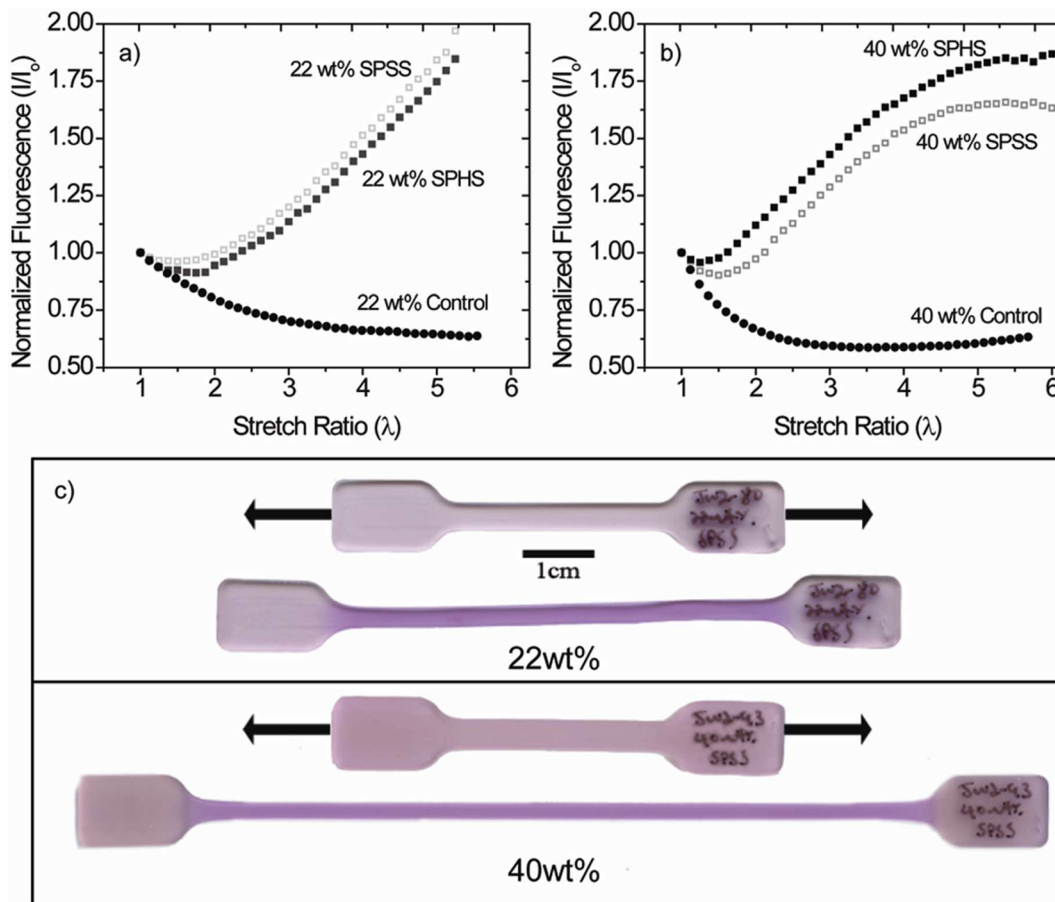


**Figure 4.** Normalized fluorescence during monotonic stretching of active and control SP-SPU in (a) 22 wt % hard segment SPU and (b) 40 wt % hard segment SPU. (c) Optical images of mechanically activated SP-SPU (SPSS) after unloading, both strained to a stretch ratio of at least 5.5 (the 22 wt % hard segment SPU was prone to slipping out of the grips at high stretch ratios). Higher strain recovery in the 22 wt % HS SPU is due to the lower hard segment content, resulting in it being more elastomeric.

the force-induced activation of SP to MC (Figure 4c). *In situ* fluorescence images were collected during SPU stretching, and normalized average fluorescence intensities ( $I/I_0$ ) were plotted against stretch ratio (Figure 4a,b). The normalized fluorescence ( $I/I_0$ ) of the active sample decreases, increases, and then, for the 40 wt % case, levels off. This nonmonotonic behavior results from specimen thickness and scattering changes during stretching. Normalized fluorescence for the nonmechanically active difunctional control SP-SPU (see Figure S2 for detailed chemistry) is assumed to remain constant during deformation and was used to quantify the strain-induced optical (primarily thickness and scattering) effects on fluorescence. When evaluating the SP to MC activation, the mechanophore is assumed to exist primarily in the SP form below a critical force and in the MC form above this critical force,<sup>13</sup> and therefore, the increasing fluorescence values with stretch represent an increasing population of mechanophore above this critical force.

**UV Activation SP-SPU.** UV activated material was used to track orientation during uniaxial deformation. The SP incorporated SPU samples were irradiated with UV light ( $\lambda = 365$  nm) prior to stretching to convert a large population of the colorless SP mechanophore to the fluorescent MC form. By monitoring the UV activated MC form, the calculated order parameters represent the average orientation of all the mechanophores in the SPU. The UV activated samples were then incrementally strained to a stretch ratio of 6. Figure 5

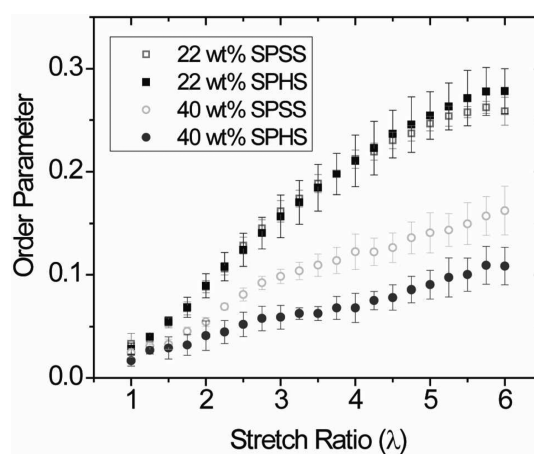


**Figure 5.** Average order parameter as a function of stretch ratio of UV activated SP-SPU. Error bars represent standard deviation of three samples tested.

shows the calculated order parameters for both compositions of hard segment with SP in the soft segment (SPSS) and SP in the hard segment (SPHS). Not surprisingly, for all samples, the order parameter under no load ( $\lambda = 1$ ) is nearly 0, indicating that the MC (i.e., from UV activation) are initially randomly oriented. The order parameters for both the 22 and 40 wt % hard segment SP-SPU samples show an increase in orientation

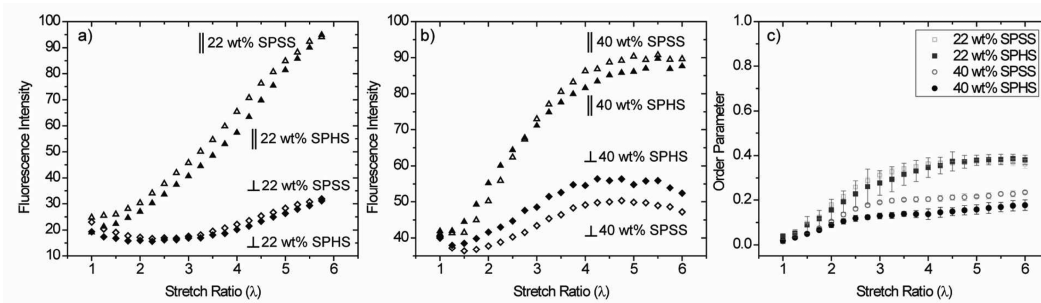


**Figure 6.** Representative parallel and perpendicular fluorescence intensities from (a) 22 and (b) 40 wt % hard segment SPSS and SPHS both stretched to a stretch ratio of at least 5.5. (c) Mechanically activated order parameter vs stretch ratio of SPSS and SPHS for both 22 and 40 wt % hard segment content SPU.

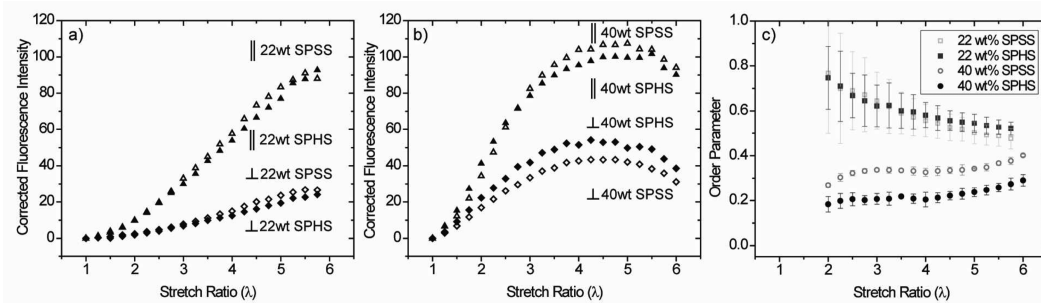


**Figure 7.** Representative corrected parallel and perpendicular fluorescence intensities for (a) 22 and (b) 40 wt % hard segment SPSS and SPHS. (c) Mechanically activated order parameters calculated from parallel and perpendicular intensities corrected for thickness and optical changes.

of the MC molecules in the direction of tensile stretch as a function of increasing stretch ratio, with the 22 wt % always more oriented than the 40 wt % hard segment material. In the 22 wt % hard segment SPU the SP in the soft and hard segments exhibit the same orientation, with order parameters increasing from near 0 to ca. 0.25 with increasing stretch ratio. The similarity between the two materials suggests that at this low quantity of hard segment the majority of the hard segment is miscible with the soft segment. The shallow and broad melting endotherm seen in Figure 2 for the 22 wt % material supports this assumption.

In the 40 wt % material, the orientation of the mechanophore also increases with stretch ratio and shows that the SPSS is always more oriented than the SPHS. The SPSS order parameter increases from near 0 to ca. 0.15, whereas the SPHS only increases to ca. 0.10 (Figure 5). The differing order parameters for SP in the two segments is consistent with the notion that these two segments are phase-separated. Assuming that orientation of the MC is directly related to the orientation and alignment of the polymer chains, the higher order parameter in the SPSS implies that rotation and alignment of the soft segment polymer chains occurs before rotation and alignment of the hard segment domains.

**Mechanically Activated SPU.** The force-induced conversion of the initially colorless SP to the fluorescent MC form was used to track orientation of the mechanophores in which force at the molecular level was sufficient to drive the SP-to-MC conversion during uniaxial deformation. Figures 6a and 6b show typical parallel and perpendicular fluorescence values for 22 and 40 wt % hard segment SPU samples. While fluorescence polarizations parallel and perpendicular to the stretch direction both increase as a function of strain, the parallel fluorescence is much higher, indicating that there are more MC mechanophores

that were mechanically activated when oriented parallel to the stretch direction relative to the perpendicular stretch direction. Using the fluorescence data in Figures 6a and 6b, order parameters were calculated and are shown in Figure 6c. The order parameters follow the same trends with stretch as in the UV activated cases.

The orientation of mechanophores at sufficient force to mechanically activate SP is somewhat obscured by the initially nonzero (and randomly oriented) fluorescence (Figures 6a and 6b). In order to isolate only the mechanically activated MC, we corrected the measured fluorescence intensities for thickness and scattering changes using the fluorescence behavior of a nonmechanically active difunctional control SP mechanophore synthesized into SPU. We assume that the thickness and optical changes during stretching of this control are similar to the active SP-SPU materials. The 22 and 40 wt % hard segment SPU corrected fluorescence intensities ( $I_{\text{mech}}$ ) isolating mechanically induced fluorescence are shown for both the SPSS and SPHS in Figures 7a and 7b. The corrected parallel and perpendicular fluorescence now start at zero and increase with stretch for both hard segment concentrations. In Figure 7b, the fluorescence appears to increase up to  $\lambda \approx 4$ , where it then levels off and then decreases. The origin of this decrease stems from the  $T_{\text{correction}}$  curve used in the fluorescence correction (see Optical Corrections section). While the fluorescence for the difunctional control samples show an overall decrease with fluorescence due to sample thinning (Figures 4a and 4b, “22 wt % Control” and “40 wt % Control”), in the 40 wt % Control around  $\lambda \approx 4$  there is a slight upturn in fluorescence. The increase in fluorescence in the 40 wt % Control at high order parameters is not fully understood but does result in the decrease in corrected fluorescence seen in Figure 7b. We believe the decrease in fluorescence at high  $\lambda$  to

be unphysical and not representative of SP mechanophore activation or orientation with mechanical force. Though the fluorescence data appear to decrease, the overall conclusions drawn from order parameter calculations, which are a ratio of the parallel and perpendicular fluorescence, are not affected. Order parameters from the isolated mechanically activated fluorescence (Figure 7c) are significantly higher than the uncorrected order parameters (Figure 6c). Order parameter values at  $\lambda < 2$  were omitted due to insufficient fluorescence. For the single phase 22 wt % hard segment SPU order parameter values range from ca. 0.7 to ca. 0.5. In the 40 wt % hard segment SPU, a clear difference in the SPSS and SPHS order parameters is still present, but now the corrected fluorescence results in greater values, ca. 0.2 to ca. 0.4.

The low glass transition temperature ( $T_g$  ca. -70 °C) and elastomeric nature of the soft segment results in a very mobile phase, while the high melting temperature ( $T_m$  ca. 160 °C) of the hard segment domains (Figure 2) results in a glassy, more constraining local environment. It is for this reason that we assume SP in the soft segments will have greater mobility than SP in the glassier hard segment, affecting the overall ability of SP mechanophores to align under stress. The high level of orientation for mechanically activated SP (Figure 7c) in the 22 wt % hard segment compared to the 40 wt % hard segment SPU may be related to the microstructure of each material. In the 22 wt % SPU, the hard segment is miscible; thus, the load is distributed equally across the hard and soft segments, and the hard segments do not constrain rotation of the SP. The high levels of orientation then result from the soft and hard segments jointly undergoing elastomeric stretching and alignment. The miscibility of the hard and soft blocks explains the similar order parameters for the 22 wt % SPHS and 22 wt % SPSS. In the 40 wt % SPU, the hard domains are likely phase separated and may not deform equivalently with the soft domains due to the difference in mobility in each segment, resulting in the possibility of hard domains constraining the rotation of the SP. And, at a given stretch ratio, more of the strain may be across the soft segments, resulting in the observed higher order parameter for the SPSS than the SPHS (Figures 6c and 7c).

The corrected mechanically activated SP-SPU order parameters also show interesting trends as a function of stretch ratio. In the UV activated cases (Figure 5), the order parameters all increased with increasing stretch ratio, representing the effect of the macroscopic deformation on the orientation of all mechanophores. The order parameters in the mechanically activated case (Figure 7c) decrease with increasing stretch ratio for the 22 wt % hard segment and only modestly increase with increasing stretch ratio in the 40 wt % hard segment SPU. The difference between the UV activated (all mechanophores activated) and the mechanically activated (only mechanophores which feel sufficient local force activated) results demonstrates the orientation-dependent effect of force on mechanophore activation. Essentially, mechanophores oriented perpendicular to the applied force are unlikely to activate, while the UV activates mechanophores regardless of orientation.

The decreasing order parameter with increasing stretch ratio seen in the 22 wt % hard segment SPU can likely be attributed to increasing levels of force at higher stretch ratios. A similar trend in mechanophore orientation was seen in elastomeric poly(methyl acrylate).<sup>16</sup> At low stretch ratios those mechanophores which are highly aligned with the direction of stretch

activate first. As the sample is strained, the stress in the SPU increases, and force across the polymer chains increases, which in turn causes mechanophores that are increasingly off-axis to also activate, lowering the overall average calculated order parameter. The trend in the 40 wt % hard segment SPU is also different than the more homogeneous 22 wt % hard segment SPU. The order parameter initially shows slight increases, plateaus from  $\lambda \approx 3$  to  $\lambda \approx 4$ , and then again increases slightly to  $\lambda = 6$ . The origins of noncontinuous changes in the order parameter in the 40 wt % SPU could be a combination of factors; we hypothesize the observation may be related to the "hard segment breakup" phenomena common in SPUs.<sup>35,36</sup> As the SPU is initially stretched, most of the deformation is likely carried by the soft segment, seen by the higher increase in order parameter for the SPSS from  $\lambda \approx 2$  to  $\lambda \approx 3$ . From  $\lambda \approx 3$  to  $\lambda \approx 4$ , deformation may become more distributed between both segments, possibly the origin of the slight plateau, and finally at  $\lambda > 4$ , the hard segment domains begin to break up due to higher levels of stress. As the hard segment domains break up, soft segment chains which were previously unstretched chains connecting hard domains can now stretch and orient, supported by the slight increase in orientation for the SPSS (Figure 7c). The slight increase in the orientation seen in the SPHS material at  $\lambda > 4$  may be due to more alignment of the SPHS because the hard domains break up in the direction of stretch.

The order parameters determined for the mechanically activated SPU samples are ratios of the parallel and perpendicular fluorescence; therefore, to determine a degree of activation for the SP mechanophore, the measured fluorescence intensities rather than the order parameters need to be compared. In the 22 wt % material, the change in fluorescence intensity with stretch ratio for both the SPSS and SPHS are about the same (Figures 6a and 7a). This similarity is evidence that the SP mechanophore at this low hard segment content is essentially in the same local environment, independent of whether SP was synthesized into the hard segment or soft segment. Therefore, at this concentration of hard segment, the SPSS and SPHS have a similar degree of mechanical activation.

Since the SPHS in 40 wt % hard segment SPU had a lower average order parameter, the SP is less mobile in the hard segment and is expected to show a lower degree of activation compared to the more aligned SPSS. Figures 6b and 7b present the 40 wt % hard segment SPU fluorescence data for the parallel fluorescence and perpendicular fluorescence for both the SPSS and SPHS. The parallel fluorescence intensity is about the same for both the SPSS and the SPHS, indicating that while the SPHS is in a less mobile environment, it does have enough mobility to mechanically activate. The degrees of activation of the SP in both the hard and soft segment are comparable when the mechanophore is oriented in the direction of stretch, but the SP in the hard segment is capable of mechanically activating at much lower levels of alignment relative to the direction of stretch. These results suggest that force is carried differently in the elastomeric soft segment and the glassy hard segment. In the elastomeric soft segment force is translated into simultaneous rotating and SP in chains that are not aligned do not activate because those chains do not carry significant force. The hard segment chains, having a higher glass transition temperature, do not undergo the same elastomeric-like chain deformation as the soft segment does. The force on the SP mechanophore causing activation in the hard segment may be

more dominated by intermolecular chain forces, allowing activation of mechanophore which are not fully aligned with the direction of stretch.

## CONCLUSION

The SP mechanophore was incorporated into either the soft or hard segment phase of segmented polyurethane and shown to be mechanochromic. Using the SP mechanophore as a molecular level probe, the orientation and force-induced activation of the mechanophore in each phase at two different hard segment compositions (22 and 40 wt %) of SPU were studied. When the SP mechanophore was synthesized into either the soft segment (SPSS) or hard segment phase (SPHS) of the 22 wt % material, the same levels of activation and orientation for both SPSS and SPHS are seen in UV activated and mechanically activated experiments, suggesting a lack of phase segregation. In the mechanically activated experiments, this single-phase material also demonstrated high levels of alignment (order parameter ca. 0.5–0.7) with the direction of stretch. In the 40 wt % hard segment material, segregation of the hard and soft segments was evident, and the SPSS and SPHS show different average order parameters as a function of increasing stretch ratio. The higher level of orientation for the SPSS in 40 wt % material compared to the SPHS suggests that the force felt by the mechanophore in each phase is different. Similar levels of fluorescence in the parallel direction indicate that while the hard segment phase is glassy, there is still enough mobility for force-induced activation of the mechanophore. The higher perpendicular fluorescence for SPHS indicates that SP mechanically activates in the hard segment at lower levels of alignment. The different mechanism by which force is transferred to the mechanophore in each phase provides insight into force distribution in each local environment.

## ASSOCIATED CONTENT

### Supporting Information

Figures S1–S3. This material is available free of charge via the Internet at <http://pubs.acs.org>.

## AUTHOR INFORMATION

### Corresponding Author

\*E-mail: pbraun@illinois.edu (P.V.B.).

### Notes

The authors declare no competing financial interest.

## ACKNOWLEDGMENTS

This work was supported by the Army Research Office MURI (Grant W011NF-07-1-0409). C.K.L. thanks Yi Chen for assistance in data collection and Enjiong Lu for material synthesis. M.N.S. thanks the Arnold and Mabel Beckman Foundation for a Beckman Fellowship.

## REFERENCES

- (1) Caruso, M. M.; Davis, D. A.; Shen, Q.; Odom, S. A.; Sottos, N. R.; White, S. R.; Moore, J. S. *Chem. Rev.* **2009**, *109*, 5755–5798.
- (2) Hickenboth, C. R.; Moore, J. S.; White, S. R.; Sottos, N. R.; Baudry, J.; Wilson, S. R. *Nature* **2007**, *446*, 423–427.
- (3) Brantley, J. N.; Wiggins, K. M.; Bielawski, C. W. *Polym. Int.* **2013**, *62*, 2–12.
- (4) Potisek, S. L.; Davis, D. A.; Sottos, N. R.; White, S. R.; Moore, J. S. *J. Am. Chem. Soc.* **2007**, *129*, 13808–13809.

- (5) Davis, D. A.; Hamilton, A.; Yang, J.; Cremar, L. D.; Van Gough, D.; Potisek, S. L.; Ong, M. T.; Braun, P. V.; Martinez, T. J.; White, S. R.; Moore, J. S.; Sottos, N. R. *Nature* **2009**, *459*, 68–72.
- (6) Kryger, M. J.; Ong, M. T.; Odom, S. A.; Sottos, N. R.; White, S. R.; Martinez, T. J.; Moore, J. S. *J. Am. Chem. Soc.* **2010**, *132*, 4558–4559.
- (7) Lenhardt, J. M.; Black, A. L.; Beiermann, B. A.; Steinberg, B. D.; Rahman, F.; Samborski, T.; Elsakr, J.; Moore, J. S.; Sottos, N. R.; Craig, S. L. *J. Mater. Chem.* **2011**, *21*, 8454–8459.
- (8) Diesendruck, C. E.; Steinberg, B. D.; Sugai, N.; Silberstein, M. N.; Sottos, N. R.; White, S. R.; Braun, P. V.; Moore, J. S. *J. Am. Chem. Soc.* **2012**, *134*, 12446–12449.
- (9) Tennyson, A. G.; Wiggins, K. M.; Bielawski, C. W. *J. Am. Chem. Soc.* **2010**, *132*, 16631–16636.
- (10) Paulusse, J. M. J.; Sijbesma, R. P. *Chem. Commun.* **2008**, 4416–4418.
- (11) Minkin, V. I. *Chem. Rev.* **2004**, *104*, 2751–2776.
- (12) Beiermann, B. A.; Davis, D. A.; Kramer, S. L. B.; Moore, J. S.; Sottos, N. R.; White, S. R. *J. Mater. Chem.* **2011**, *21*, 8443–8447.
- (13) Lee, C. K.; Davis, D. A.; White, S. R.; Moore, J. S.; Sottos, N. R.; Braun, P. V. *J. Am. Chem. Soc.* **2010**, *132*, 16107–16111.
- (14) Kingsbury, C. M.; May, P. A.; Davis, D. A.; White, S. R.; Moore, J. S.; Sottos, N. R. *J. Mater. Chem.* **2011**, *21*, 8381–8388.
- (15) O'Bryan, G.; Wong, B. M.; McElhanon, J. R. *ACS Appl. Mater. Interfaces* **2010**, *2*, 1594–1600.
- (16) Beiermann, B. A.; Kramer, S. L. B.; Moore, J. S.; White, S. R.; Sottos, N. R. *ACS Macro Lett.* **2012**, *1*, 163–166.
- (17) Bletz, M.; Pfeifer-Fukumura, U.; Kolb, U.; Baumann, W. *J. Phys. Chem. A* **2002**, *106*, 2232–2236.
- (18) Hepburn, C. *Polyurethane Elastomers*; Applied Science Publishers: London, 1982.
- (19) Petrović, Z. S.; Ferguson, J. *Prog. Polym. Sci.* **1991**, *16*, 695–836.
- (20) Miller, J. A.; Lin, S. B.; Hwang, K. K. S.; Wu, K. S.; Gibson, P. E.; Cooper, S. L. *Macromolecules* **1985**, *18*, 32–44.
- (21) Rubner, M. F. *Macromolecules* **1986**, *19*, 2114–2128.
- (22) Rubner, M. F. *Macromolecules* **1986**, *19*, 2129–2138.
- (23) Nallicheri, R. A.; Rubner, M. F. *Macromolecules* **1991**, *24*, 517–525.
- (24) Stanford, J. L.; Young, R. J.; Day, R. J. *Polymer* **1991**, *32*, 1713–1725.
- (25) Koevoets, R. A.; Karthikeyan, S.; Magusin, P. C. M. M.; Meijer, E. W.; Sijbesma, R. P. *Macromolecules* **2009**, *42*, 2609–2617.
- (26) Hammond, P. T.; Nallicheri, R. A.; Rubner, M. F. *Mater. Sci. Eng., A* **1990**, *126*, 281–287.
- (27) Kim, S.-J.; Reneker, D. H. *Polym. Bull.* **1993**, *31*, 367–374.
- (28) Crenshaw, B. R.; Weder, C. *Chem. Mater.* **2003**, *15*, 4717–4724.
- (29) Crenshaw, B. R.; Weder, C. *Macromolecules* **2006**, *39*, 9581–9589.
- (30) Gurp, M. *Colloid Polym. Sci.* **1995**, *273*, 607–625.
- (31) Baur, G.; Stieb, A.; Meier, G. *Mol. Cryst. Liq. Cryst.* **1973**, *22*, 261–269.
- (32) Damerau, T.; Hennecke, M. *J. Chem. Phys.* **1995**, *103*, 6232.
- (33) Li, Y.; Ren, Z.; Zhao, M.; Yang, H.; Chu, B. *Macromolecules* **1993**, *26*, 612–622.
- (34) Leung, L. M.; Koberstein, J. T. *J. Polym. Sci., Polym. Phys. Ed.* **1985**, *23*, 1883–1913.
- (35) Yeh, F.; Hsiao, B. S.; Sauer, B. B.; Michel, S.; Siesler, H. W. *Macromolecules* **2003**, *36*, 1940–1954.
- (36) Sup Lee, H.; Ra Yoo, S.; Won Seo, S. *J. Polym. Sci., Part B: Polym. Phys.* **1999**, *37*, 3233–3245.